Anomalous itinerant-electron metamagnetic transition in the layered $Sr_{1-x}Ca_xCo_2P_2$ system

Masaki Imai,[1,*] Chishiro Michioka,[1] Hiroto Ohta,[2] Akira Matsuo,[3] Koichi Kindo,[3]
Hiroaki Ueda,[1] and Kazuyoshi Yoshimura[1,4,†]

[1]*Department of Chemistry, Graduate School of Science, Kyoto University, Kyoto 606-8502, Japan*
[2]*Department of Applied Physics, Tokyo University of Agriculture and Technology, Koganei, Tokyo 184-8588, Japan*
[3]*Institute for Solid State Physics, The University of Tokyo, Kashiwanoha, Kashiwa, Chiba 277-8581, Japan*
[4]*Research Center for Low Temperature and Materials Sciences, Kyoto University, Kyoto 606-8502, Japan*

(Received 7 February 2014; revised manuscript received 23 June 2014; published 10 July 2014)

Magnetic properties of the layered itinerant system $Sr_{1-x}Ca_xCo_2P_2$ were investigated under a magnetic field up to 70 T. As for the exchange-enhanced Pauli paramagnetic metal $SrCo_2P_2$, the magnetization curve shows two characteristic anomalies. The high-field anomaly corresponds to an itinerant-electron metamagnetic transition (IEMT), while the low-field one is small and broad without any obvious hystereses just as the crossover phenomenon between different energy states. Such a successive transition in the magnetization curve cannot be explained by the conventional phenomenological theory for IEMT based upon the Landau expansion of the magnetic free energy, but by the extended Landau expansion theory dealing with two distinguishable energy states. In the systematical study on $Sr_{1-x}Ca_xCo_2P_2$, furthermore, the metamagnetic transition field decreases and goes to zero as x increases up to 0.5, indicating that the ferromagnetic quantum critical point exists at $x \sim 0.5$.

DOI: 10.1103/PhysRevB.90.014407 PACS number(s): 75.10.Lp, 75.30.Kz, 75.45.+j

I. INTRODUCTION

More than 500 layered AT_2X_2-type compounds (A: alkaline metal, alkaline-earth metal, lanthanide; T: transition metal; X: metalloid) with the $ThCr_2Si_2$ structure (space group: $I4/mmm$) have been discovered so far [1], and found to show a wide variety of interesting physical properties such as the heavy-fermion superconductivity in $CeCu_2Si_2$ [2], the high-T_c superconductivity and nematic hidden ordering in $Ba_{1-x}K_xFe_2As_2$ and $BaFe_2(As_{1-x}P_x)_2$ [3,4], as well as the itinerant-electron ferromagnetism in $LaCo_2P_2$ [5,6]. These properties are highly related to their quasi-two-dimensional (2D) electronic structure, in which the electronic correlation with low-dimensional fluctuation effects becomes so strong that the exotic electronic phenomena would be realized.

The crystal structure of AT_2X_2 is formed by stacks of A and T_2X_2 layers alternately and has two types of the interlayer staking bond depending on A and X: one leads to the collapsed tetragonal (cT) structure and the other to the uncollapsed tetragonal (ucT) one, which are categorized by the strength of the X-X chemical bond between neighboring T_2X_2 layers [7]. In the case of the ucT compound, T_2X_2 layers are well isolated and their electronic structures are expected to have strong two dimensionality, while in the case of the cT compound, a strong interlayer interaction would induce three-dimensional characters. Therefore, the strength of the X-X bond would be a key for controlling the dimensionality and physical properties of the AT_2X_2 compound.

Since it is known that the structure changes from ucT to cT around $x = 0.5$ as x increases in the $Sr_{1-x}Ca_xCo_2P_2$ system [8], this system should be one of the ideal systems to control the dimensionality of the magnetic interaction and the itinerancy systematically. The $SrCo_2P_2$ with the ucT cell is an exchange-enhanced Pauli paramagnetic compound without any magnetic orderings [9]. In the ucT region ($x \leqslant 0.5$) in which the electronic structure is expected to be quasi-2D, the Weiss temperature changes from negative value to 0 K with increasing x, suggesting that $Sr_{1-x}Ca_xCo_2P_2$ approaches a ferromagnetic quantum critical point (QCP). In the cT region ($x > 0.5$) in which $Sr_{1-x}Ca_xCo_2P_2$ shows magnetic orderings [8], the intralayer ferromagnetic moments are coupled antiferromagnetically via layer-by-layer P-P bondings.

In this paper, we show an itinerant-electron metamagnetic transition (IEMT) in the $Sr_{1-x}Ca_xCo_2P_2$ system, interpret their characteristic magnetization curves by means of the extended Landau expansion theory, and discuss the itinerant-electronic state in the quasi-2D transition metal pnictide system.

II. EXPERIMENTAL METHOD

Single crystalline and polycrystalline samples of $Sr_{1-x}Ca_xCo_2P_2$ were prepared from Sr(2N), Ca(2N5), Co(3N), and P(red, 5N). The single crystals with $x = 0$ and 1 were obtained by a tin flux method [5]. High quality polycrystalline samples were synthesized through the following steps. First, SrP, CaP, and Co_2P were synthesized by heating stoichiometric mixtures of the pure elements. The obtained SrP, CaP, and Co_2P powders were mixed in the ratio of $1.2x$:$1.2(1-x)$:1.0. The mixture was pelletized and sealed into an evacuated silica tube and then heated up to 1000 °C. To obtain high homogeneities, we repeated this process at least twice. Excess SrP and CaP were dissolved in water.

X-ray diffraction patterns were measured using Cu $K\alpha$ radiation, and refined by the Le Bail method, using a computer program RIETAN-FP [10]. The temperature-dependent magnetizations of $Sr_{1-x}Ca_xCo_2P_2$ were measured by a Quantum Design MPMS-XL system at the Research Center for Low Temperature and Materials Sciences, Kyoto University. Magnetization curves beyond 70 T were measured by using an induction method with a multilayer pulsed magnet at the ultrahigh magnetic field laboratory of the Institute for Solid State Physics, the University of Tokyo. Field swept ^{31}P NMR spectra

*m.imai@kuchem.kyoto-u.ac.jp
†kyhv@kuchem.kyoto-u.ac.jp

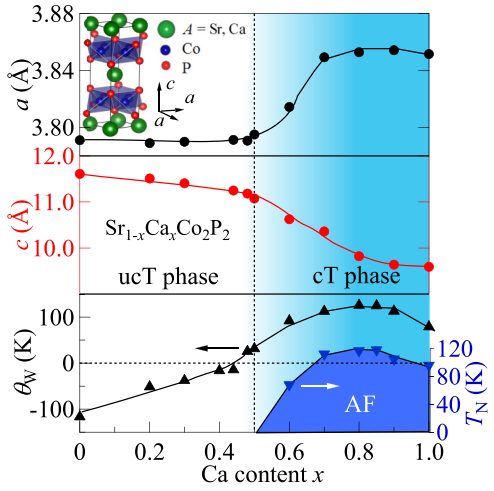

FIG. 1. (Color online) Lattice parameters and magnetic properties of $Sr_{1-x}Ca_xCo_2P_2$. Lattice parameters a and c are shown in the upper and middle panels, respectively. The Weiss and Néel temperatures are shown in the bottom panel. Here, the unit cell of $Sr_{1-x}Ca_xCo_2P_2$ is shown in the inset, and AF stands for the antiferromagnetic state.

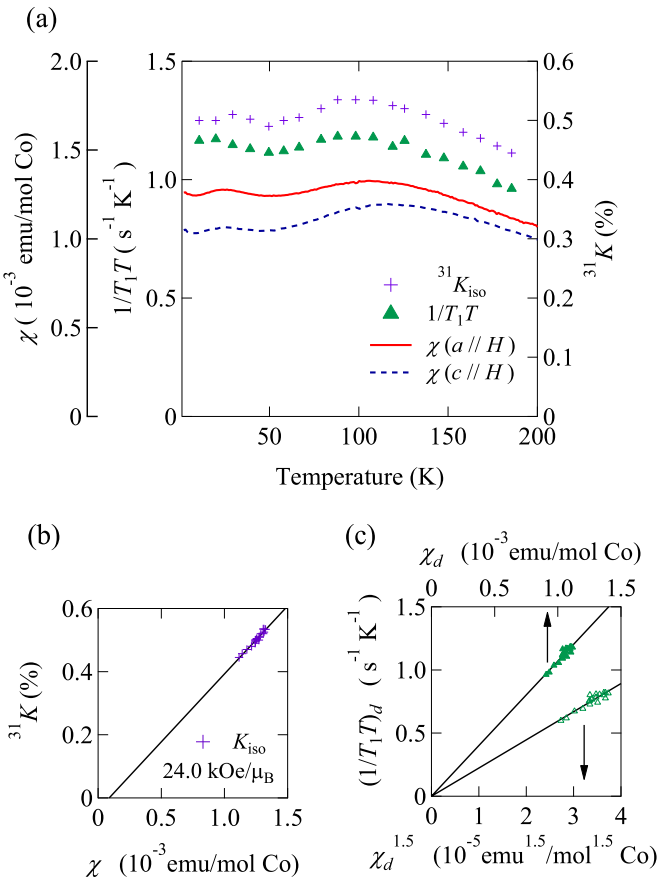

FIG. 2. (Color online) Temperature dependence of the static and dynamical magnetic susceptibility of $SrCo_2P_2$. The dashed line and the solid line show the magnetic susceptibility of single crystals with the magnetic field along a and c, respectively. The open circles shows the Knight shift of the ^{31}P NMR study of the polycrystalline sample, reflecting the spin susceptibility of metals. The solid triangles stand for $1/T_1T$.

were measured by the spin-echo method by using a coherent pulse spectrometer. The ^{31}P nucleus has a nuclear spin $I = 1/2$ and a gyromagnetic ratio $^{31}\gamma = 1.7237$ MHz/kOe. The Knight shift ^{31}K was obtained as $^{31}K = (H_{\rm ref} - H_{\rm res})/H_{\rm res}$, where $H_{\rm ref} = \nu_{\rm ref}/^{31}\gamma$ with the operating frequency $\nu_{\rm res}$ of 29.800 MHz. The nuclear spin-lattice relaxation rate $1/T_1$ was measured by the inversion-recovery method for the echo signal after an inversion π pulse at the maximum position of the spectrum, and the nuclear magnetization recovery was found to follow a simple single exponential for $I = 1/2$ at all the temperatures.

III. RESULTS AND DISCUSSION

Lattice parameters a and c of $Sr_{1-x}Ca_xCo_2P_2$ determined from x-ray diffraction measurements are shown in Fig. 1. In the ucT region of $x \leqslant 0.5$, a is almost constant, while c decreases monotonically. Since the parameter c is linearly related to the P-P distance between neighboring Co_2P_2 layers [8], the interlayer couplings in the quasi-2D electronic structure are enhanced with decreasing c, i.e., the P-P distance. Around $x = 0.5$, a and c show marked changes according to the lattice collapse driven by forming P-P bonds between neighboring Co_2P_2 layers. With further increase of x, c decreases and a increases in the cT region. It is known that the first-order structural phase transition from the ucT to the cT phase occurs due to the P-P binding energy barrier in the ACo_2P_2 system including $EuCo_2P_2$, which shows the transition under the physical pressure [11]. In this system, the energy barrier is just around $x = 0.5$ and causes first-order-like rapid variations of lattice parameters.

In Fig. 2, we show the magnetic properties of $SrCo_2P_2$. The temperature dependence of magnetic susceptibility $\chi(T)$ shows anomalous double maxima at 25 and 110 K. In general, the magnetic susceptibility χ, Knight shift K, and $1/T_1T$ are decomposed as

$$\chi(T) = \chi_d(T) + \chi_{\rm orb} + 2/3\chi_{\rm CE} + \chi_{\rm dia}, \quad (1)$$

$$K(T) = K_d(T) + K_{\rm orb} + K_{\rm CE}, \quad (2)$$

$$1/T_1T = (1/T_1T)_d + (1/T_1T)_{\rm orb} + (1/T_1T)_{\rm CE} + (1/T_1T)_{\rm dia}, \quad (3)$$

where the subscripts d, orb, CE, and dia represent d electron spin, d electron orbital, conduction electron, and diamagnetic components, respectively. Here, we can assume that only the d spin component depends on T while other terms are constant. In the ^{31}P NMR study, K and $1/T_1T$ also show a similar temperature dependence of $\chi(T)$, which supports that the double-peak anomalies originate in its intrinsic spin susceptibility. The K vs χ plot in Fig. 2(b), therefore, does show a linear relation with a slope, i.e., the hyperfine coupling constant of 24.0 kOe/μ_B. The width of the NMR spectrum does not change markedly between 4.2 and 200 K (not shown). Furthermore, in the nuclear spin-lattice relaxation rate $1/T_1$, no anomaly corresponding to the magnetic ordering was observed. These results suggest that $SrCo_2P_2$ has no magnetic ordering.

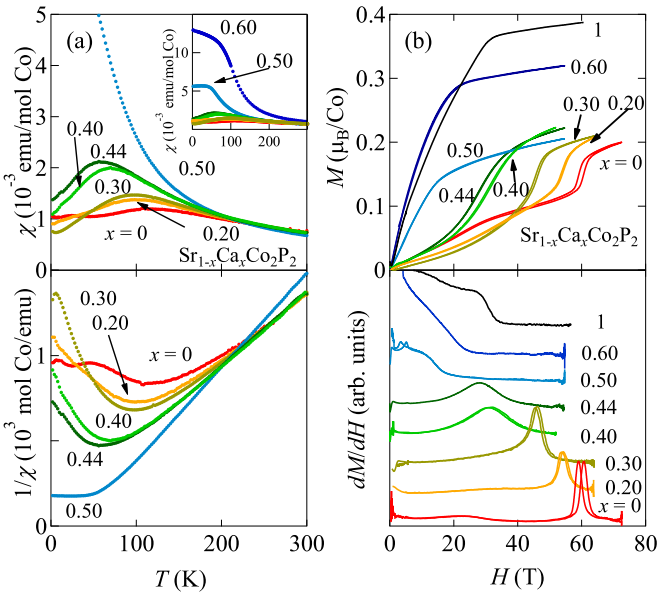

FIG. 3. (Color online) Magnetic properties of $Sr_{1-x}Ca_xCo_2P_2$. (a) The magnification figure for the temperature dependence of the magnetic susceptibility χ and its inverses $1/\chi$ (inset: full scale figure). The susceptibility χ shows maximum behaviors in the region of $0 \leqslant x \leqslant 0.5$ without any magnetic orderings, and the maximum temperature decreases as x increases. (b) The magnetization M and the differential magnetization dM/dH curves measured at 4.2 K in pulsed high magnetic fields up to 70 T.

According to the self-consistent renormalization theory of spin fluctuations, $1/T_1T$ reflects the dynamical susceptibility [12]. Figure 2(c) shows the linear relationship between $1/T_1T$ and $\chi^{1.5}$, which indicates that $SrCo_2P_2$ has quasi-2D ferromagnetic spin fluctuations [13]. Such a behavior is distinguishable from the antiferromagnetic case, in which $1/T_1T$ is correlated with the staggered spin susceptibility $\chi_{\boldsymbol{q}}$ enhanced around the antiferromagnetic q vector $\boldsymbol{q} = \boldsymbol{Q}$.

The static susceptibility $\chi(T)$ often shows a maximum at a finite temperature in the case of nearly itinerant ferromagnetic compounds [14–17]. However, the appearance of double-peak anomalies is unique behavior in this compound.

The temperature dependence of the magnetic susceptibility $\chi(T)$ of $Sr_{1-x}Ca_xCo_2P_2$ is shown in Fig. 3(a). For all the compositions, $\chi(T)$ shows a Curie-Weiss-like temperature dependence at high temperatures. The Weiss temperature θ_W determined by fitting $\chi(T)$ with the Curie-Weiss formula is plotted in the lower panel of Fig. 1. In the case of the itinerant-electron magnets, the origin of the Curie-Weiss-like behavior is attributed to the temperature dependence of the amplitude of the local spin fluctuation (spin density), and an apparent negative Weiss temperature does not always mean the existence of antiferromagnetic interactions [12]. In the case of the itinerant magnetism with ferromagnetic spin fluctuations, θ_W indicates the distance from the quantum critical point with $\theta_W = 0$ [18,19]. For example, nearly ferromagnetic metals such as Pd, YCo_2, $LuCo_2$, and $Sr_{1-x}Ca_xRuO_3$ also exhibit Curie-Weiss-like temperature dependence with negative θ_W's [14,20–23]. In the $Sr_{1-x}Ca_xCo_2P_2$ system, θ_W increases from negative to 0 as x increases from 0 to 0.5, suggesting that ferromagnetic spin fluctuations are enhanced and the system approaches the QCP.

In the case of nearly ferromagnetic compounds, $\chi(T)$ often shows a maximum at a finite temperature [14–17]. In some compounds of $Sr_{1-x}Ca_xCo_2P_2$, $\chi(T)$ shows double maxima. In the end compound with $x = 0$, the lower maximum temperature T_{max1} and the higher maximum temperature T_{max2} are 25 and 110 K, respectively. In the NMR study shown in Fig. 2(a), such behaviors are found to be intrinsic. For $x = 0.2$, T_{max1} and T_{max2} are 30 and 97.5 K, respectively. For $0.3 \leqslant x \leqslant 0.5$, T_{max2} becomes lower as x increases and T_{max1} disappears. For $0.6 \leqslant x$, the ground state becomes antiferromagnetic with antiferromagnetic interlayer couplings due to the enhanced interlayer P-P bonding. In this region, the value of θ_W is positive in spite of the antiferromagnetic ground state. This fact is due to the strong intralayer ferromagnetic couplings.

The magnetization M and its differential dM/dH curves of $Sr_{1-x}Ca_xCo_2P_2$ at 4.2 K are shown in Fig. 3(b). For $x = 0$, with increasing applied magnetic field H, an anomaly as a broad maximum in the dM/dH vs H curve appears at $H_{c1} = 23$ T, and then an obvious and sharp peak is observed at $H_{c2} = 59.7$ T as shown in the lower panel of Fig. 3(b). The latter anomaly looks like a typical behavior of the itinerant electron metamagnetic transition (IEMT) as in the case of $Co(S, Se)_2$ [24], $Y(Co, Al)_2$ [17,25,26], and $(Fe, Co)_3Mo_3N$ [27,28]. The IEMT is a transition from the Pauli paramagnetic state without any obvious magnetic moments and magnetic orderings to the itinerant ferromagnetic state, and is completely different from the metamagnetic transitions of localized moment systems such as spin flip/flop phenomena. A hysteresis loop in M-H curves suggests the present IEMT is a first-order transition. For $x = 0.2$, although the anomaly at $H_{c1} = 33$ T is so small and broad, similar behaviors are observed as in the magnetization curve for $x = 0$. For $0.3 \leqslant x \leqslant 0.5$, only a single clear anomaly corresponding to IEMT at H_{c2} is observed systematically. The critical field H_{c2} becomes lower and the anomaly becomes blunt as x increases. With increasing x, H_{c1} becomes higher and then seems to merge with H_{c2}. Within the ucT region of $0 \leqslant x \leqslant 0.5$, the saturation magnetic moment is about $0.2\mu_B$ in all the compounds. On the other hand, in the case of the compounds with $x = 0.6$ and 1 which have the cT structure, the saturation magnetization is 0.3 and $0.4\mu_B$ and larger than that in the ucT compounds. The electronic state of P changes from isolated P^{3-} to diatomic P_2^{4-} with the lattice collapse [7]. As a result, the hypothetical valence of Co or the number of the electrons in the $3d$ band changes and the local spin density on Co becomes larger. From above systematical studies, we obtain the magnetic phase diagram as shown in Fig. 4(a).

In order to explain the IEMT in the present case, let us now introduce the Wohlfarth-Rhodes-Shimizu (WRS) theory [29,30], giving the explanation of IEMT with the Landau expansion of the free energy, in which the free energy can be written with the magnetic moment M and the external field H as

$$F = F_0 + \frac{1}{2}AM^2 + \frac{1}{4}BM^4 + \frac{1}{6}CM^6 - MH, \qquad (4)$$

$$H = \frac{\partial}{\partial M}F = AM + BM^3 + CM^5. \qquad (5)$$

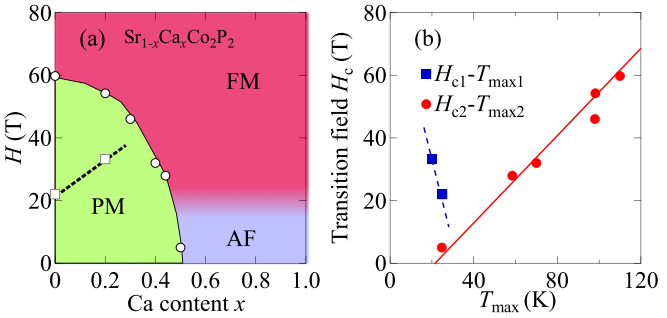

FIG. 4. (Color online) (a) Magnetic phase diagram of $Sr_{1-x}Ca_xCo_2P_2$ at 4.2 K. PM: the paramagnetic state; AF: the antiferromagnetic state; FM: the field-induced ferromagnetic state. (b) The relation between the maximum temperatures in χ-T curves T_{max} and the metamagnetic transition fields H_c in the $Sr_{1-x}Ca_xCo_2P_2$ system.

Here A, B, and C are the expansion coefficients originating in the electron density of states and its derivatives at the Fermi level. The conditions among coefficients for the occurrence of the first-order IEMT and the crossover from the paramagnetic to ferromagnetic states are respectively written as

$$A > 0,\ B < 0,\ C > 0, \quad \text{and} \quad \frac{3}{16} < \frac{AC}{B^2} < \frac{9}{20} \quad \text{(IEMT)}, \tag{6}$$

$$A > 0,\ B < 0,\ C > 0, \quad \text{and} \quad \frac{AC}{B^2} \geqslant \frac{9}{20} \quad \text{(crossover)}. \tag{7}$$

Yamada [31] developed the WRS theory taking spin fluctuations into account and succeeded in explaining the maximum behavior in the temperature dependence of $\chi(T)$, which was frequently observed in nearly ferromagnetic itinerant-electron metamagnets [14–17] as well as present cases. Although the above model based on the Landau expansion is quite simple, it succeeded in explaining the single-step IEMT. However, this theory cannot explain our results, in which the magnetization curve shows double anomalies. Trying to explain double anomalies within this model, we must require the expansion to be at least up to the M^{10} term instead of the M^6 term, since the triple minima are needed in its free energy. However, it is not so reasonable or so realistic. This model employs the free energy of a single state described by Eq. (4). It is equivalent to the assumption that the band structure does not change in the paramagnetic and ferromagnetic states. Excluding this assumption, Takahashi and Sakai introduced a theoretical model started from two almost degenerated electronic states [32]. In some metamagnetic compounds such as Y(Co, Al)$_2$ and La(Fe, Si)$_{13}$, their band structures and spin fluctuation parameters are changed through the metamagnetic transition, and lattice parameters also change through the magnetovolume effect [14,33,34]. Therefore, using two different states with different band structures, i.e., with different spin fluctuation parameters as well as with the different magnetovolume effect seems to be quite reasonable. We introduce the model assuming two states (state 1 and 2), and use up to the sixth expansion term in their free energies. Here, the free energies of state 1, $F_1(M)$, and state 2, $F_2(M)$, are

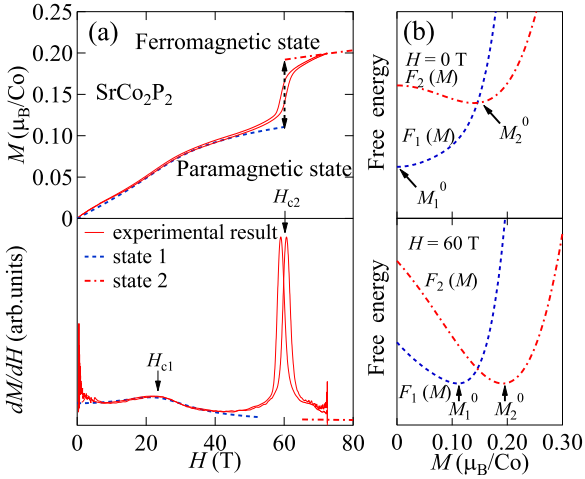

FIG. 5. (Color online) (a) Experimental and simulated magnetization curves and their differentials of $SrCo_2P_2$. (b) Schematic free energy curves in the condition of $H = 0$ and 60 T. The ground state changes from the paramagnetic to ferromagnetic state when $F_1(M) = F_2(M)$. The solid line shows the experimental result, and dashed-dotted and dashed lines are simulated magnetizations of states 1 and 2 with $A = 4000$ kOe/μ_B, $B = 6.0\times10^4$ kOe/μ_B^3, $C = 1.0\times10^7$ kOe/μ_B^5, $A' = -2500$ kOe/μ_B, $B' = 1.5\times10^5$ kOe/μ_B^3, and $C' = 0$ kOe/μ_B^5.

written as

$$F_1(M) = F_1(0) + \tfrac{1}{2}AM^2 + \tfrac{1}{4}BM^4 + \tfrac{1}{6}CM^6 - MH, \tag{8}$$

$$F_2(M) = F_2(0) + \tfrac{1}{2}A'M^2 + \tfrac{1}{4}B'M^4 + \tfrac{1}{6}C'M^6 - MH, \tag{9}$$

with $A > 0$, $B < 0$, $C > 0$, $A' < 0$, and $C' \geqslant 0$, respectively. Figure 5(a) shows the magnetization and differential magnetization curves simulated by utilizing the above functions and the experimental curves of $SrCo_2P_2$ for comparison. As a result, the simulated curves can reproduce the small anomaly at H_{c1} and the first-order IEMT at H_{c2}. We show a schematic free energy diagram of the present model in Fig. 5(b). The free energy curves of $F_1(M)$ and $F_2(M)$ show a minimum at M_1^0 and M_2^0, respectively, and the magnetization in the ground state is $M_1^0 = 0$ with state 1 at zero field. Under the external field, state 2 is relatively stabilized. Consequently as a result, the first-order metamagnetic transition comes from the phase transition from state 1 to 2 at H_{c2}, where $F_1(M_1^0) = F_2(M_2^0)$ is satisfied. The metamagnetic transition field H_{c2} depends on the value of $\Delta F(0) = F_2(0) - F_1(0)$.

The anomaly at the lower field H_{c1} for $x = 0$ and 0.2 occurs when the expansion parameters in the free energy for state 1 in Eq. (8) satisfy the relation in Eq. (7). Therefore, the anomaly is a kind of crossover behavior under the external field from the ground state ($M = 0$) to a somewhat higher magnetization state ($M \neq 0$). In this case, because the change of the electronic state is quite small, the characteristics within the state 1 model should be enough to explain the experiment and one does not need to divide states through the crossover. Moreover, the present two-states model can explain the double maxima behavior of $\chi(T)$ and the relation between T_{max} and H_c. Here, we discuss the temperature dependence of the free

energy. State 1 is the ground state in the low-temperature region, and then the initially metastable state 2 is stabilized with increasing temperature and becomes the lowest energy state above T_{max}, where $F_1(0,T_{max}) \geqslant F_2(0,T_{max})$ is satisfied. Because both H_c and T_{max} are proportional to $\Delta F(0)^{1/2}$, H_c and T_{max} are predicted to show a linear relationship [35]. As shown in Fig. 4(b), H_{c2} is almost proportional to T_{max}, consistent with the prediction. Note that in the case of $x = 0$ and 0.2, there are two anomalies both in the temperature dependence of the magnetic susceptibility and in the magnetization curve. The lower-temperature maximum at T_{max1} is explained by the temperature dependence of expansion coefficients of $F_1(H,T)$ as well as the crossover in the magnetization curve.

The simulated parameters of states 1 and 2 are written in the caption of Fig. 5. Takahashi and Sakai's theory requires that these two states are almost degenerated. If our simulated result for the difference in energies between state 1 and 2 is out of theoretical requirements, it may be due to the contribution of the two-band nature. In any case, if two states have quite different magnetizations, one should treat them using separable free energies.

Next we will discuss the x dependence. Similar saturation moments in the ucT region for $x \leqslant 0.5$ suggest that the band structure of state 2 does not change markedly with x. According to the above model, $\Delta F(0)$ decreases with the Ca substitution x as well as the metamagnetic transition field. In this system, the lattice collapse along the c axis with the Ca substitution enhances the interlayer correlation of the electronic structure. This fact is the reason why the intralayer Co moments order ferromagnetically and the interlayer Co moments do antiferromagnetically in the cT region.

Considering the fact that all magnetically ordered ACo_2P_2 have ferromagnetically ordered planes [5,36], cobalt moments in an ab plane generally have the ferromagnetic interaction in this system. The interlayer interaction leads to various interlayer magnetic structures.

In the present case of the $Sr_{1-x}Ca_xCo_2P_2$ system, a ferromagnetic QCP is found to lie around $x = 0.5$ in this system as shown in Figs. 1 and 4(a). The first-order-like lattice collapse transition from the ucT to cT phases occurs at almost the same point ($x = 0.5$), and antiferromagnetic orderings take place at the ground state in the cT region ($x > 0.5$) by interlayer interactions through the P-P bonding. In the ucT region ($x < 0.5$), the interaction along the c axis is very weak and the two-dimensional ferromagnetic interaction in the ab plane is dominant. Then, the ferromagnetic interactions are found to increase by the Ca substitution, which is an opposite phenomenon of the usual effect with the band narrowing. In this system, the following two possibilities are candidates as the origin of the enhancement of the ferromagnetic interaction. The first candidate is the increase of carrier density at a mainly cobalt contributed band by the decrease of the interlayer P-P distance and the Co-P coupling, and the second one is the suppression of spin fluctuations, which disturb magnetic orderings, by the interlayer interactions through the P-P coupling.

IV. CONCLUSION

In summary, we have found the metamagnetic transitions and the ferromagnetic quantum criticality in $Sr_{1-x}Ca_xCo_2P_2$ ($x \leqslant 0.5$) with the quasi-2D ucT cell. Specifically, the compounds with $x = 0$ and 0.2 show two maxima in the temperature dependence of the magnetic susceptibility. These two anomalies have the same origin with the two anomalies in the magnetization curve, i.e., the crossover and the IEMT phenomena, which cannot be explained by the conventional WRS theory. We succeed in quantitatively explaining our results with the extended model assuming two separated states. The present results are expected to lead to a breakthrough in the research field of itinerant magnetism, especially in the investigation of metamagnetism in the quasi-2D itinerant system.

ACKNOWLEDGMENT

This work is supported by Grants-in-Aid for Scientific Research Grants No. 22350029 and No. 23550152 from the Ministry of Education, Culture, Sports, Science and Technology of Japan and Grants for Excellent Graduate Schools, MEXT, Japan.

[1] CRYSTMET®5.0.0, The Metals Database, Toth Information System Inc., 2013.
[2] F. Steglich, J. Aarts, C. D. Bredl, W. Lieke, D. Meschede, W. Franz, and H. Schäfer, Phys. Rev. Lett. **43**, 1892 (1979).
[3] M. Rotter, M. Tegel, and D. Johrendt, Phys. Rev. Lett. **101**, 107006 (2008).
[4] S. Kasahara, H. J. Shi, K. Hashimoto, S. Tonegawa, Y. Mizukami, T. Shibauchi, K. Sugimoto, T. Fukuda, T. Terashima, Andriy H. Nevidomskyy, and Y. Matsuda, Nature (London) **486**, 382 (2012).
[5] M. Reehuis, C. Ritter, R. Ballou, and W. Jeitschko, J. Magn. Magn. Mater. **138**, 85 (1994).
[6] M. Imai, C. Michioka, H. Ohta, H. Ueda, and K. Yoshimura, J. Jpn. Soc. Powder Powder Metallurgy. **61**(S1), S60 (2014).
[7] R. Hoffmann and C. Zheng, J. Phys. Chem. **89**, 4175 (1985).
[8] S. Jia, A. J. Williams, P. W. Stephens, and R. J. Cava, Phys. Rev. B **80**, 165107 (2009).
[9] E. Mörsen, B. D. Mosel, W. Müller-Warmuth, M. Reehuis, and W. Jeitschko, J. Phys. Chem. Solids **49**, 785 (1988).
[10] F. Izumi and K. Momma, Solid State Phenom. **130**, 15 (2007).
[11] M. Chefki, M. M. Abd-Elmeguid, H. Micklitz, C. Huhnt, W. Schlabitz, M. Reehuis, and W. Jeitschko, Phys. Rev. Lett. **80**, 802 (1998).
[12] T. Moriya, *Spin Fluctuations in Itinerant Electron Magnetism* (Springer-Verlag, New York, 1985).
[13] M. Hatatani and T. Moriya, J. Phys. Soc. Jpn. **64**, 3434 (1995).
[14] K. Yoshimura, M. Mekata, M. Takigawa, Y. Takahashi, and H. Yasuoka, Phys. Rev. B **37**, 3593 (1988).
[15] T. Goto, Y. Shindo, H. Takahashi, and S. Ogawa, Phys. Rev. B **56**, 14019 (1997).
[16] M. Takigawa and H. Yasuoka, J. Phys. Soc. Jpn. **51**, 787 (1982).

[17] T. Sakakibara, T. Goto, K. Yoshimura, K. Murata, and K. Fukamichi, J. Magn. Magn. Mater. **90-91**, 131 (1990).
[18] Y. Takahashi, J. Phys. Soc. Jpn. **55**, 3553 (1986).
[19] T. Moriya, J. Magn. Magn. Mater. **100**, 261 (1991).
[20] K. Yoshimura, T. Shimizu, M. Takigawa, H. Yasuoka, and Y. Nakamura, J. Phys. Soc. Jpn. **53**, 503 (1984); K. Yoshimura, K. Fukamichi, H. Yasuoka, and M. Mekata, *ibid.* **56**, 3652 (1987).
[21] F. E. Hoare and J. C. Matthews, Proc. R. Soc. London, Ser. A **212**, 137 (1952).
[22] T. Kiyama, K. Yoshimura, K. Kosuge, H. Mitamura, and T. Goto, J. Phys. Soc. Jpn. **68**, 3372 (1999).
[23] K. Yoshimura, T. Imai, T. Kiyama, K. R. Thurber, A. W. Hunt, and K. Kosuge, Phys. Rev. Lett. **83**, 4397 (1999).
[24] K. Adachi, K. Sato, M. Matsuura, and M. Ohashi, J. Phys. Soc. Jpn. **29**, 323 (1970).
[25] T. Sakakibara, T. Goto, K. Yoshimura, M. Shiga, and Y. Nakamura, Phys. Lett. A **117**, 243 (1986).
[26] T. Sakakibara, T. Goto, K. Yoshimura, and K. Fukamich, J. Phys.: Condens. Matter **2**, 3381 (1990).
[27] T. Waki, Y. Umemoto, S. Terazawa, Y. Tabata, A. Kondo, K. Sato, K. Kindo, S. Alconchel, F. Sapiña, Y. Takahashi, and H. Nakamura, J. Phys. Soc. Jpn. **79**, 093703 (2010).
[28] T. Waki, S. Terazawa, T. Yamazaki, Y. Tabata, K. Sato, A. Kondo, K. Kindo, M. Yokoyama, Y. Takahashi, and H. Nakamura, Europhys. Lett. **94**, 37004 (2011).
[29] E. P. Wohlfarth and P. Rhodes, Philos. Mag. **7**, 1817 (1962).
[30] M. Shimizu, J. Phys. (Paris) **43**, 155 (1982).
[31] H. Yamada, Phys. Rev. B **47**, 11211 (1993).
[32] Y. Takahashi and T. Sakai, J. Phys.: Condens. Matter **7**, 6279 (1995).
[33] H. Wada, K. Yoshimura, G. Kido, M. Shiga, M. Mekata, and Y. Nakamura, Solid State Commun. **65**, 23 (1988).
[34] A. Fujita, Y. Akamatsu, and K. Fukamichi, J. Appl. Phys. **85**, 4756 (1999).
[35] Y. Takahashi and T. Sakai, J. Phys.: Condens. Matter **10**, 5373 (1998).
[36] M. Reehuis, W. Jeitschko, G. Kotzyba, B. Zimmer, and X. Hu, J. Alloys Compd. **266**, 54 (1998).